Eur. Phys. J. D **34**, 67–71 (2005)
DOI: 10.1140/epjd/e2005-00121-x

THE EUROPEAN PHYSICAL JOURNAL D

The dissociation energy of V_{13}^+ and the consequences for radiative cooling

K. Hansen[1,a], A. Herlert[2], L. Schweikhard[2], M. Vogel[3], and C. Walther[4]

[1] Department of Physics, Göteborg University, 41296 Göteborg, Sweden
[2] Institut für Physik, Ernst-Moritz-Arndt-Universität Greifswald, Domstr. 10a, 17487 Greifswald, Germany
[3] Institut für Physik, Johannes Gutenberg-Universität Mainz, 55099 Mainz, Germany
[4] Institut für Nukleare Entsorgung, Forschungszentrum Karlsruhe, Postfach 3640, 76021 Karlsruhe, Germany

Received 6 September 2004
Published online 13 July 2005 –

Abstract. The dissociation energy of V_{13}^+ has been determined by comparison of the rates of sequential fragmentation, $V_{13}^+ \rightarrow V_{12}^+ \rightarrow V_{11}^+$, and single-step fragmentation of the first fragment, $V_{12}^+ \rightarrow V_{11}^+$. The dissociation-energy value obtained as $D = 4.35(13)$ eV has implications for the amount of radiative cooling of the cluster derived form the data presented earlier [C. Walther et al., Phys. Rev. Lett. **83**, 3816 (1999)] and is used to analyze additional results.

PACS. 36.40.Vz Optical properties of clusters – 44.40.+a Thermal radiation – 82.80.Ms Mass spectrometry (including SIMS, multiphoton ionization and resonance ionization mass spectrometry, MALDI)

1 Introduction

Highly excited, free clusters of metallic materials can decay through a number of different channels, e.g., the emission of fragments with sizes from a single atom to small molecules, the emission of electromagnetic radiation (radiative cooling) or of an electron (thermionic emission), and fission–like processes in the case of multiply charged clusters. Decay processes involving particle emission have already been extensively studied, both for gas phase molecules and clusters. Fragmentation of clusters can be observed under a number of experimental conditions; it frequently occurs spontaneously in molecular beams, it can be induced by electron impact ionization or by absorption of photons, in collisions with atoms, molecules and surfaces, when the clusters are exposed to a thermal heat bath or combinations of these excitation methods [1–7]. The emission of atoms and dimers reflects the separation energies for the processes and, with some modeling, this has allowed a large amount of information to be collected about e.g. electronic and geometrical shell effects [8–10].

Radiative cluster cooling has already been observed for a number of refractory metals [11,12]. Broad cluster size distributions were usually used except for the case of V_{13}^+ [13]. When measured, the emission spectra are smooth and resemble the Planck spectrum [12]. A large number of radiative cooling experiments have also been performed for the easily size-selected fullerenes, i.e., for C_{60} [15–17], $C_{N<60}^+$ [18], C_{60}^+ [17,19,20], and C_{60}^- [21] with, however, broad thermal distributions. The observed cooling rates of fullerenes are in general higher than expected on the basis of IR-active modes alone [21,22]. Radiative cooling has been studied for other finite size systems as well, such as organic molecules [23,24]. In the model used in [24], the cooling is assumed to originate exclusively from a single harmonic radiator mode. In analogy to the fullerenes, we expect that the radiation of metal clusters will be dominated by electronic contributions, originating in the tail of the plasmon excitation [25].

In contrast to the decays involving loss of particles, cooling by photon emission does not lead to changes of the mass or the charge of a cluster. This feature renders radiative cooling more difficult to investigate in quantitative detail unless special experimental techniques are applied. The technique used here is to measure the influence of the radiative cooling on another decay channel which is more easily measured. The channel chosen is the statistical, unimolecular loss of a single atom. The presence of radiative cooling can be inferred from the data described below without any modelling, but a more quantitative description requires that some parameters of the unimolecular decay are known.

In reference [13] the first radiative cooling measurements were reported for size-selected metal clusters, V_{13}^+, at well defined excitation energies. The choice of V_{13}^+ as probe object was based on several experimental criteria: a refractory material allows access to high temperatures; a mono-isotopical element eases the contaminant-free ion-selection, and the 13 atom cluster fits with respect to

[a] e-mail: klavs@fy.chalmers.se

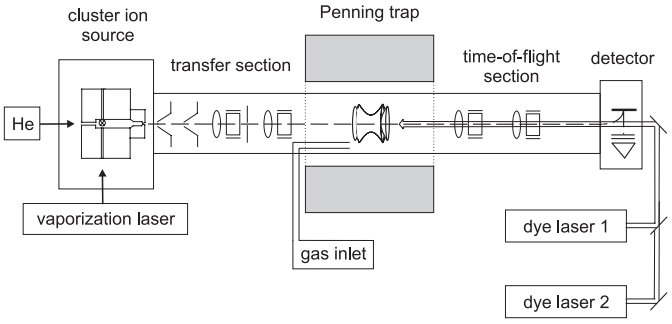

Fig. 1. Schematic drawing of the experimental set-up.

restrictions posed by the availability of photon energies and observation time windows. Recently, experiments on vanadium clusters have been performed by use of far-infrared spectroscopy [14] and a high symmetry was found for V_{13}^+. The implications for the present study are not yet clear.

In [13] the data were compared with Monte-Carlo simulations of the competing radiative and unimolecular decays based on a modified Planck-emission law. To this end the cooling rate as well as the dissociation energy were taken as free parameters. With a recently developed method [26,27] the dissociation energy of V_{13}^+ has now been determined in an independent measurement. In the following this study is presented and its consequences with regard to the earlier investigations on the competition between fragmentation and radiative cooling are discussed.

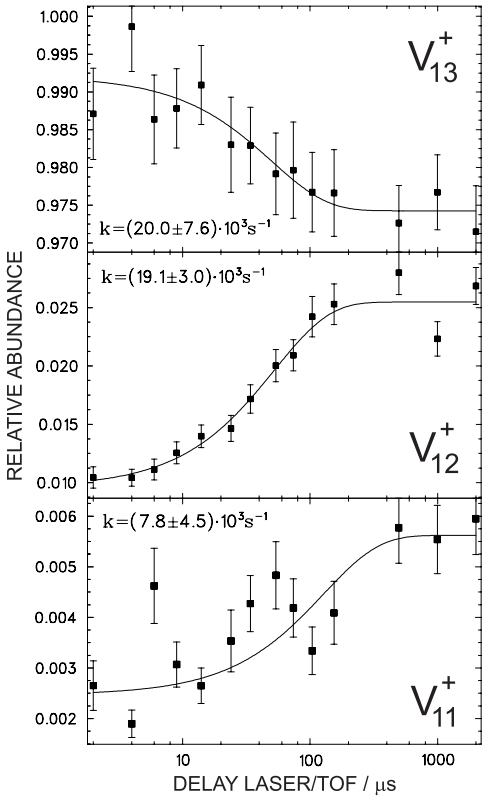

Fig. 2. Relative abundances of V_{13}^+, V_{12}^+, and V_{11}^+ as a function of the delay time between photoexcitation ($h\nu = 3.85$ eV) and ejection for TOF mass-analysis.

2 Experimental set-up and procedure

The cluster trap combines an external ion source with a Penning trap and a time-of-flight (TOF) mass spectrometer ([28] and references therein). A schematic drawing of the set-up is shown in Figure 1. The clusters are produced in a Smalley-type laser vaporization source: The light of a pulsed, frequency doubled Nd:YAG laser (5–10 mJ, 10 ns) ablates material from a vanadium wire. The desorbed material, captured by a simultaneously released helium jet, is expanded adiabatically into the vacuum. The process produces small neutral, anionic and cationic clusters. For the present study the positively charged clusters are guided towards a Penning trap [29] which consists of a superposition of two static fields: a homogeneous magnetic field for radial confinement is provided by a superconducting magnet and an electric quadrupolar field for axial confinement is created by hyperbolically shaped ring and endcap electrodes. Mass selection of V_{13}^+ is accomplished by resonant radial ejection of all other ions.

The V_{13}^+ clusters are centered by a combination of buffer gas collisions and quadrupolar excitation [30] and confined within a region of about 1.8 mm diameter in the middle of the trap [31]. Before storage, the clusters are cooled by the helium gas in the source, and in the storage process the clusters undergo an estimated additional 300 collisions with argon atoms. The result is equilibration to a canonical ensemble at the trap (room) temperature. The thermalization has been checked previously on gold clusters of similar size [26]. The internal energy of the vanadium clusters is found by scaling of the thermal properties of bulk vanadium [13], which gives a total internal energy of $E_0 = 0.53(14)$ eV. The thermal spread of ± 0.14 eV, from the room temperature canonical ensemble, is the only width in pre-decay internal energy that needs to be considered, even after photoexcitation.

The excitation laser system comprises two Nd:YAG pumped dye lasers, providing 10-ns pulses at a repetition rate of 10 Hz, and single pulses are selected by means of two mechanical shutters. Both beams are guided axially through the vacuum apparatus including the Penning trap (see Fig. 1). After laser irradiation, followed by a variable delay time Δt the charged reaction products are axially ejected into the drift section for time-of-flight mass analysis. The data of 200 cycles (with 20 to 50 V_{13}^+ clusters each) are added to obtain statistically significant signal intensities.

3 Method and results

Because all charged products are detected, not only the decrease of the precursor V_{13}^+, but also the corresponding increase of fragments is observed: in Figure 2 the relative yields of V_{13}^+, V_{12}^+ and V_{11}^+ are plotted as function of storage time after laser irradiation. The solid lines represent

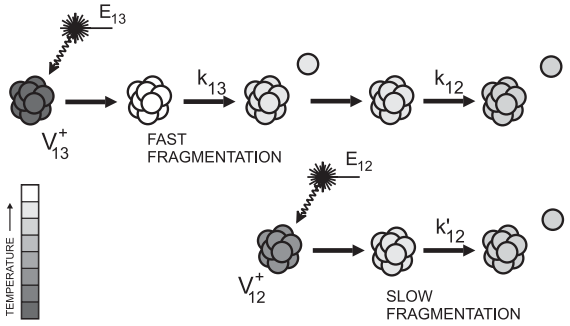

Fig. 3. Sketch of the decay schemes for the determination of the dissociation energy. Top: sequential decay of V_{13}^+. Bottom: single-step decay of V_{12}^+.

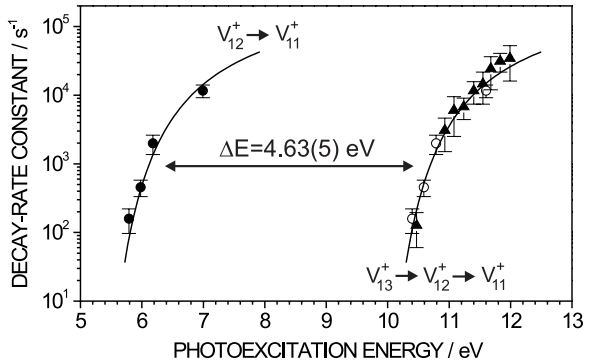

Fig. 4. Decay-rate constants for the direct decay of V_{12}^+ into V_{11}^+ (full circles) and V_{13}^+ into V_{11}^+ (full triangles) as a function of the photoexcitation energy. The solid lines is an simultaneous fit to both data sets (see text). For comparison the data points of the direct decay are shifted by the energy difference of $\Delta E = 4.63(5)$ eV onto the curve of the sequential decay (open circles).

fits of the exponentials

$$N_{13} = a - b\,e^{-k\Delta t} \tag{1}$$

$$N_i = a' + b\,e^{-k\Delta t}, \qquad i = 11, 12 \tag{2}$$

to the data, yielding a good agreement of precursor decrease (top) and buildup of V_{12}^+ (middle). In addition, the relative yield of V_{11}^+ clusters increases with delay time, but with a different rate constant. These ions are produced via sequential evaporation of two atoms. The V_{13}^+ clusters evaporate a first atom on a time-scale too short to be resolved by the experimental set-up. However, after the first decay, the resulting V_{12}^+ clusters are hot enough to emit a second atom. This happens at a considerably longer time scale which allows the time-resolved observation of the decay.

When combined with an independent measurement of the one-step decay of V_{12}^+ to V_{11}^+, this yields a model-free determination of the dissociation energy of V_{13}^+, as described in [26,27]. The sequential decay

$$V_{13}^+ \xrightarrow{k_{13}} V_{12}^+ \xrightarrow{k_{12}} V_{11}^+ \tag{3}$$

is compared to the direct process

$$V_{12}^+ \xrightarrow{k'_{12}} V_{11}^+, \tag{4}$$

where k_{13} and k_{12} are the rate constants of the first and the second fragmentation steps, respectively (see Fig. 3). The second step can be monitored time-resolved. The rate constant k'_{12} of the direct process (4) serves as a calorimeter or effectively an uncalibrated thermometer for the last step of the sequential reaction (3). When the decay-rate constant for V_{12}^+ is the same in both reactions, i.e. $k_{12} = k'_{12}$, then the energy content of the V_{12}^+ is the same in both reactions and thus the dissociation energy of the V_{13}^+ is given by [26,27]

$$D = E_{13} - E_{12} + \Delta E_{th} - E_{KER}, \tag{5}$$

where $\Delta E_{th} = 0.05$ eV is the difference in the initial thermal energy, E_{KER} the (small) kinetic energy that is released in the first step of the sequential reaction, and E_{13} and E_{12} are the photoexcitation energies for the sequential and single-step decay, respectively. Several decay-rate constants were measured as a function of excitation energy. They are plotted as solid symbols in Figure 4. The solid lines result from a simultaneous fit to the decay-rate constants of the sequential and the direct processes with an Arrhenius-like function $k(E) = a\exp(-b/(c+E))$. They differ only by a constant shift in energy of $\Delta E = D + E_{KER} - \Delta E_{th} = 4.63(5)$ eV. At first glance the uncertainty from the simultaneous fit is surprisingly small. This is due to the corresponding steep increase of χ^2 as a function of a small shift in the distance between the two curves. The fit of the shift was repeated with several slightly different procedures — all of which led to very similar results within the given statistical uncertainty.

To extract the dissociation energy, the kinetic energy release during the reaction $V_{13}^+ \rightarrow V_{12}^+$, E_{KER}, needs to be subtracted. This is a stochastic number and the effect of the width of this distribution on the measured rate constants needs in principle to be calculated. But the width is expected to be small and does not exceed the thermal width of the precursor cluster. We will therefore use the average value of the E_{KER}. It is calculated as the average of the kinetic energy distribution, as described in [32,33] and the value is 0.33(12) eV. The uncertainty is conservatively estimated relative to earlier value, because of the uncertainty in the caloric curve which is an adjustable function here. In summary this translates into a dissociation energy of $D = 4.35(13)$ eV, which is in agreement with an independent result, $D = 4.65(32)$ eV, from collisional induced dissociation measurements [34].

Note that the present determination of D is insensitive to radiative cooling in the first evaporation step [32]. At the present excitation energies radiative cooling takes place on time scales of the order of several tens of microseconds or slower [13]. Hence, only the second, slow fragmentation step of the sequential dissociation will be affected by photon emission. However, the influence is the same for the direct fragmentation rate and any effects cancel when equation (5) is applied. In contrast, radiative cooling becomes important when the fragmentation is compared to

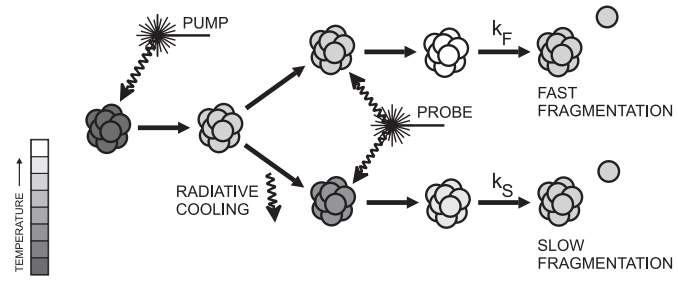

Fig. 5. Schematic experimental sequence for detection of radiative cooling.

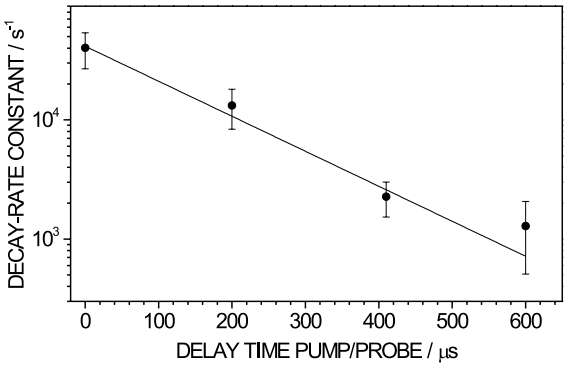

Fig. 6. Decay-rate constant of V_{13}^+ as a function of the delay between the pump ($h\nu = 5.4$ eV) and the probe laser pulse ($h\nu = 2.3$ eV). The solid line is an exponential fit to the data.

a statistical model without using such a 'thermometer'-reaction. For the single-step decays described above the precursor clusters were excited by absorption of two photons, which not necessarily were absorbed simultaneously but at least within the duration of the laser pulse (10 ns). The radiative cooling then takes place as a competing process to the fragmentation.

In order to separate the two reactions in time the pump-probe scheme sketched in Figure 5 has been applied [13]. The clusters are excited again by two photons, but now these are provided by separate laser pulses. This opens the possibility to tune the energy of the photons independently from each other and it allows to control the time, ΔT, between the two excitation events. After the second laser pulse the products are detected at a variable delay time Δt, and the fragment buildup is observed time resolved as described in the previous paragraph. The important advantage is the decoupling of radiative cooling and fragmentation: by absorption of the pump photon ($h\nu = 5.4$ eV), the cluster is excited to an energy just above the fragmentation threshold (see Fig. 5), where atom evaporation is very slow ($k < 1000$ s^{-1}) and radiative cooling becomes dominant. After a delay period ΔT a second photon (probe-pulse) provides additional energy and the cluster fragments fast (Fig. 5, top). If the cluster loses energy by emitting a photon during the time between the laser pulses its remaining energy falls short of the sum of both quanta and the fragmentation proceeds more slowly (Fig. 5, bottom). The internal energy of the cluster is thus probed via the fragmentation rate. The present investigation complements the earlier studies of reference [13] where instead of the decay-rate constants only the fragment yields at a fixed time (of 20 ms) after the probe pulse were monitored.

The presence of radiation can be inferred from the data without any modelling. In the absence of radiation the delay between the pump and probe laser pulse will not affect the total excitation energy in the cluster after the second photon absorbed and thus the rate will be independent of the delay, in contrast to the observed behavior. The cooling process is of statistical nature and only a decreasing mean energy of the cluster ensemble is measured. More precisely, one observes a superposition of many rate constants. Figure 6 shows the data discussed here. V_{13}^+ is fragmented by two photons, a pump photon of $h\nu = 5.4$ eV followed by a probe photon of $h\nu = 2.3$ eV. For each data point the delay ΔT between pump and probe pulse is kept constant and the rate of the decay is determined as presented in Figure 2 and described above. Within 600 μs the cluster cools by an amount of energy causing the dissociation rate to decrease by one order of magnitude.

4 Discussion

A straightforward interpretation of these data is difficult for several reasons, due to both the number of processes but mainly the number of potentially unknown parameters in the problem, like the heat capacity of the clusters, the emissivity, etc. This complicated situation has previously been modelled numerically by Monte Carlo simulations [13].

As an alternative we have treated the data in Figure 6 with a simplified model. It consists of a photon emission rate constant and an expression for the unimolecular rate constant as used in [13], which is based on detailed balance [33]. The former is adapted from [25] and represents the radiation as emanating from the low energy tail of the surface plasmon resonance. In the relevant low energy limit, the expression for the spectral photon emission rate constant simplifies to

$$A' d\omega = \frac{12\omega^4 \gamma r_n^3}{\pi \omega_{ps}^2 c^3} \frac{e^{-\hbar\omega/k_B T(E-\hbar\omega/2)}}{1 - e^{-\hbar\omega/k_B T(E-3\hbar\omega/2)}} d\omega, \qquad (6)$$

where ω is the angular frequency, γ the damping of the resonance, ω_{ps} is the surface plasmon frequency, and c is the speed of light. The radius for a cluster of n atoms is $r_n = r_s n^{1/3} + r_0$ with the Wigner-Seitz radius $r_s = 1.48$ Å. A spill-out of $r_0 = \hbar/\sqrt{2 m_e W} = 0.95$ Å has been assumed, where $W = 4.2$ eV is the bulk work function of vanadium. The surface plasmon energy is given by $\hbar\omega_{ps} = \hbar\omega_p/\sqrt{3} = 6.93$ eV where the plasmon frequency ω_p is related to the electron density $n_e = N/V_n$ by $\omega_p = \sqrt{e^2 n_e/(\epsilon_0 m_e)}$ with the number of valence electrons $N = 3n - 1$ and the volume of the cluster $V_n = (4/3)\pi r_n^3$.

The temperature in equation (6) is the microcanonical temperature [35], which was calculated according to the

recipe given in [13]. The fraction involving the exponential factors requires that the absorption cross-section is independent of temperature [36] as has been experimentally shown for V_{13}^+ in the visible region [37]. The width of the plasmon resonance is kept as a free parameter and is parametrized with the dimensionless parameter s, i.e. $\gamma = s\,\omega_p$. With the reference value $s = 1$, the emitted power at 6.93 eV is calculated by integration of equation (6) to $P_{rad}(s = 1, E = 6.93\,\mathrm{eV}) = 1.08 \times 10^5\ \mathrm{eVs}^{-1}$. It changes a factor of 2 over ca. 1 eV which is a modest change compared with the change in unimolecular rate constant, and we will therefore use the constant value above.

With the dissociation energy $D = 4.35$ eV as reported above, the unimolecular rate constant at $\Delta T = 0$ is higher than the observed $4 \times 10^4\,\mathrm{s}^{-1}$. We adjusted the heat capacities of precursor and product clusters in order to bring the calculated values into agreement with the experimental value for the rate constant. The correction consisted of increasing the a and b coefficients in the caloric curve (essentially the heat capacity) [13] by a factor 1.17, which is not an unreasonable value. The rate constant then has a logarithmic derivative of $3.45\ \mathrm{eV}^{-1}$ at the total energy of $E = E_{pump} + E_{probe} + E_0 = 8.23$ eV. This value is not very sensitive to the scaling of the heat capacities. The scaling was also used for the photon emission rate constant and it changed the value a factor 2 downwards. The decrease in unimolecular rate constant with pump-probe delay ΔT is then given by

$$\frac{d\ln(k(8.23\,\mathrm{eV}))}{d\Delta T} = \frac{d\ln(k(8.23\,\mathrm{eV}))}{dE}\left(-P(s, 6.93\,\mathrm{eV})\right) = s\frac{d\ln(k(8.23\,\mathrm{eV}))}{dE}\left(-P(s = 1, 6.93\,\mathrm{eV})\right). \quad (7)$$

Inserting the above values yields

$$\frac{d\ln(k(8.23\,\mathrm{eV}))}{d\Delta T} = s\,3.7 \times 10^5\ \mathrm{s}^{-1}. \quad (8)$$

This is to be compared with the experimental result shown in Figure 6. A weighted exponential fit (solid line) gives $6.8 \times 10^3\,\mathrm{s}^{-1}$. This translates into $s = 0.018$, and thus a width of the plasmon of $\hbar\gamma = 0.12$ eV, or a FWHM of 0.24 eV. Note that this value is not necessarily identical to the one determined from the shape of the resonance close to the centroid, but is rather the parameter that describes the low energy part of the dielectric function.

The relevance of the dissociation energy in this evaluation is most easily seen if the rate constant is expressed in terms of the microcanonical temperature [35] with an Arrhenius-type expression. The logarithmic derivative of k in equation (7) is then seen to be proportional to D. Hence the right hand side of equation (7) is proportional to $s\,D$, and the independent determination of D then fixes the value of s, i.e. γ.

5 Conclusion

By comparison of the sequential decay of V_{13}^+ and the single-step decay of V_{12}^+ the dissociation energy of V_{13}^+ has been determined: $D = 4.35(13)$ eV. The uncertainty is dominated by the uncertainty of the kinetic energy release in the process. The present value is about 1 eV smaller than inferred from a Monte-Carlo simulation in a previous investigation [13], but in agreement with an independent result from collisional induced dissociation measurements [34].

The data from measurements on the radiative cooling of the cluster have been fitted with a model based on the surface plasmon resonance. The single free parameter in the fit was the width of the resonance, $\hbar\gamma = 0.12$ eV. The analysis involved several approximations and the value of γ is not necessarily the ultimate number. The magnitude is, however, reasonable, and we consider it a confirmation of the parametrization of the radiation.

This work was supported by the European Cluster Cooling Network under the contract (HPRN-CT-2000-00026), and the Swedish National Research Council (VR).

References

1. W.D. Knight et al., Phys. Rev. Lett. **52**, 2141 (1984)
2. O. Echt et al., Phys. Rev. Lett. **47**, 1121 (1981)
3. M.F. Jarrold et al., J. Chem. Phys. **86**, 3876 (1987)
4. C.-X. Su et al., J. Chem. Phys. **99**, 6506 (1993)
5. C. Bréchignac et al., J. Chem. Phys. **101**, 6992 (1994)
6. S. Krückeberg et al., J. Chem. Phys. **110**, 7216 (1999)
7. M. Schmidt et al., Phys. Rev. Lett. **79**, 99 (1997)
8. M. Brack, Rev. Mod. Phys. **65**, 677 (1993)
9. T.P. Martin, Phys. Rep. **273**, 199 (1996)
10. J. Borggreen et al., Phys. Rev. A **62**, 013202 (2000)
11. R. Scholl et al., in *Physics and Chemistry of Finite Systems: From Clusters to Crystals*, NATO ASI, Ser. C, Vol. 374 (Kluwer Academic, New York, 1992), p. 1275
12. U. Frenzel et al., Chem. Phys. Lett. **240**, 109 (1995)
13. C. Walther et al., Phys. Rev. Lett. **83**, 3816 (1999)
14. A. Fielicke et al., Phys. Rev. Lett. **93**, 023401 (2004)
15. R. Mitzner et al., J. Chem. Phys. **103**, 2445 (1995)
16. E. Kolodney et al., Phys. Rev. Lett. **74**, 510 (1995)
17. A.A. Agarkov et al., Eur. Phys. J. D **9**, 331 (1999)
18. K. Hansen et al., J. Chem. Phys. **104**, 5012 (1996)
19. J. Laskin et al., Chem. Phys. Lett. **277**, 564 (1997)
20. J. Lemaire et al., Int. J. Mass Spectrom. **189**, 93 (1999)
21. J.U. Andersen et al., Phys. Rev. Lett. **77**, 3991 (1996)
22. J.U. Andersen et al., Eur. Phys. J. D **17**, 189 (2001)
23. R.C. Dunbar, Mass Spectrom. Rev. **11**, 309 (1992)
24. G.T. Uechi et al., J. Chem. Phys. **98**, 7888 (1993)
25. J.U. Andersen et al., Eur. Phys. J. D **11**, 413 (2000)
26. M. Vogel et al., Phys. Rev. Lett. **87**, 013401 (2001)
27. M. Vogel et al., J. Phys. B **36**, 1073 (2003)
28. L. Schweikhard et al., Eur. Phys. J. D **24**, 137 (2003)
29. L.S. Brown et al., Rev. Mod. Phys. **58**, 233 (1986)
30. G. Savard et al., Phys. Lett. A **158**, 247 (1991)
31. C. Walther et al., Z. Phys. D **38**, 51 (1996)
32. M. Vogel et al., Phys. Rev. A **66**, 033201 (2002)
33. K. Hansen, Philos. Mag. B **79**, 1413 (1999)
34. C.-X. Su et al., J. Chem. Phys. **99**, 6613 (1993)
35. J.U. Andersen et al, J. Chem. Phys. **114**, 6518 (2001)
36. J.U. Andersen et al., J. Phys. B **35**, R1 (2002)
37. C. Walther et al., Eur. Phys. J. D **9**, 455 (1999)